

Radial bias in face identification

Alexia Roux-Sibilon^{1,2}, Carole Peyrin², John A. Greenwood³, & Valérie Goffaux^{1,4}

¹ Psychological Sciences Research Institute (IPSY), UC Louvain, Louvain-la-Neuve, Belgium

² Univ. Grenoble Alpes, Univ. Savoie Mont Blanc, CNRS, LPNC, 38000, Grenoble, France

³ Department of Experimental Psychology, University College London, London WC1H 0AP, United Kingdom

⁴ Institute of Neuroscience (IONS), UC Louvain, Brussels, Belgium,

Abstract

Human vision in the periphery is most accurate for stimuli that point towards the fovea. This so-called radial bias has been linked with the organisation and spatial selectivity of neurons at the lowest levels of the visual system, from retinal ganglion cells onward. Despite evidence that the human visual system is radially biased, it is not yet known whether this bias persists at higher levels of processing, or whether high-level representations are invariant to this low-level orientation bias. We used the case of face identity recognition to address this question. The specialized high-level mechanisms that support efficient face recognition are highly dependent on horizontally oriented information, which convey the most useful identity cues in the fovea. We show that face selective mechanisms are more sensitive on the horizontal meridian (to the left and right of fixation) compared to the vertical meridian (above and below fixation), suggesting that the horizontal cues in the face are better extracted on the horizontal meridian, where they align with the radial bias. The results demonstrate that the radial bias is maintained at high-level recognition stages and emphasize the importance of accounting for the radial bias in future investigation of visual recognition processes in peripheral vision.

Keywords: Radial Bias; Peripheral Vision; Face identification; Orientation; Horizontal tuning.

Introduction

The retina of various species, including humans, is spatially inhomogeneous. It consists of a small fovea with high resolution capacity, and a large peripheral zone with spatial resolution decreasing as the distance from fovea increases (Baden et al., 2020; Strasburger et al., 2011). Around the fovea, retinal ganglion cells are organized in a radial manner, with elliptically shaped dendritic fields whose longer axis points toward the fovea (like the petals of a daisy flower). Due to this anatomical property, these cells maximally respond to orientations that point towards fixation (Leventhal & Schall, 1983; Schall et al., 1986). Neurophysiological studies have documented the existence of radial biases in the lateral geniculate nucleus (Shou et al., 1986; Smith et al., 1990) and in the visual cortex of cats and macaques (Leventhal, 1983; Leventhal et al., 1984; Pigarev et al., 2002; Pigarev & Rodionova, 1998; Rodionova et al., 2004). These studies describe cells with radially oriented receptive fields in areas V1 to V4. Neuroimaging studies have further corroborated the existence of a radial bias at the cortical level by showing that radial orientations elicit stronger BOLD response in retinotopic areas V1 to V3 in both humans and monkeys (Sasaki et al., 2006). Population receptive fields in V1, V2 and V3 have also been found to be radially elongated (Merkel et al., 2018, 2020; Silson et al., 2018), though these findings have been disputed (Lerma-Usabiaga et al., 2021).

The radial bias is also found at the perceptual level. Psychophysical experiments in humans have demonstrated that visual performance in peripheral vision is biased in favour of radial orientations: Sensitivity to simple stimuli such as lines or gratings is higher when they are oriented radially (see Gabor patches in Fig.1) than tangentially. For example, sensitivity on the horizontal meridian is better for a horizontal bar than for a vertical bar, and vice versa on the vertical meridian. This effect has been demonstrated with experiments measuring sensitivity to contrast (Bennett & Banks, 1991; Berardi & Fiorentini, 1991; Sasaki et al., 2006; Zheleznyak et al., 2016), spatial frequency thresholds (Rovamo et al., 1982; Venkataraman et al., 2016), phase and orientation discrimination (Bennett & Banks, 1991, Davey & Zanker, 1998), as well as Vernier and bisection acuity (Westheimer, 2003; Yap et al., 1987). The radial bias also influences saccade landing errors (Greenwood et al., 2017), as well as spatial integration mechanisms such as visual crowding, where flankers positioned radially induce more crowding than those positioned tangentially (Greenwood et al., 2017; Strasburger et al., 2011; Toet & Levi, 1992). Surround suppression in the periphery is also stronger between gratings that are arranged radially than tangentially (Malavita et al., 2018; Petrov & McKee, 2006). The radial bias adds to other well-described spatial inhomogeneities in peripheral sensitivity. Indeed, visual performance (e.g.,

contrast sensitivity or spatial resolution) is better along the horizontal than the vertical meridian independently of stimulus orientation (horizontal-vertical anisotropy); it is also better in the upper than lower visual field (vertical meridian anisotropy; Abrams et al., 2012; Himmelberg et al., 2020; see Barbot et al., 2021, for a graphical summary of these anisotropies). Unlike these other anisotropies, the radial bias is a property of orientation encoding, which adds to the overall variations in visual sensitivity across the visual field.

These past findings suggest that the radial bias is a ubiquitous feature of human vision, influencing the low and mid-level visual processing stages of the visual system (from retina to V4). However, it is not yet known whether and how this bias influences visual recognition; i.e. the ability to make higher-level semantic judgments regarding our visual environment (e.g. recognizing the identity of a given face, categorizing an artefact as a chair). Visual recognition presumably arises at high-level processing stages of the visual hierarchy. These high-level recognition stages are thought to produce complex representations that reflect the stable properties of the object, irrespective of accidental characteristics of its retinal projection, such as where the object appears in the visual field (e.g. DiCarlo et al., 2012; Leopold et al., 2001; Riesenhuber & Poggio, 1999; Schwarzlose et al., 2008). Thus, it is possible that early retinotopic biases do not affect visual recognition. Alternatively, low- to mid-level radial biases could transfer to higher-level stages of visual processing and affect visual recognition performance. The latter case assumes that the lower-level computations give more weight to radially oriented content. The representation of a peripheral object available to later stages of visual processing can thus be thought as being “radially filtered” (as schematized in Fig. 1-A). Hence, visual recognition of complex and ecologically relevant stimuli may be modulated by the position of the object in the visual field, depending on the relevance of the information conveyed by the radially-filtered orientation band.

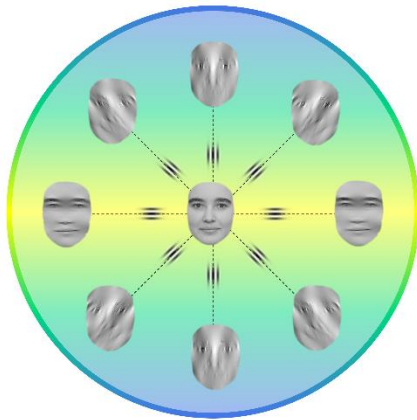
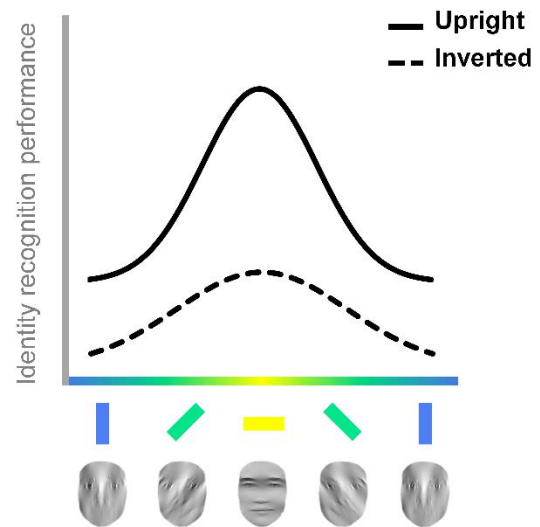
A**B**

Figure 1. A. Schematic of the radial filter hypothesis. The Gabor patches represent radial orientations (those that align with meridians), for which visual sensitivity is the best in peripheral vision. As peripheral objects (e.g. faces) are processed by radially biased receptive fields at low-level processing stages, the radially oriented content should be weighted higher in their neural representation. By this reasoning, the filtered faces schematize the information that would be propagated to the high-level processing stages specialized in the recognition of face identity. **B.** Cartoon illustration of the horizontal tuning of face identity recognition at fovea (adapted from Goffaux & Greenwood, 2016). Foveal sensitivity to face identity is highest in the horizontal range. The inversion of the face in the picture plane (dotted line) strongly reduces this horizontal tuning, revealing the importance of the horizontal content for the recruitment of face specialized processing.

In this study, we addressed whether and how radial biases survive at higher-level processing stages through the lens of human face identity recognition, making use of its strong dependence on orientation. Indeed, a number of studies conducted in foveal vision have provided consistent evidence that the visual mechanisms specialized for human face recognition are mainly driven by the horizontal content of the face image (e.g., Dakin & Watt, 2009; Duncan et al., 2019; Goffaux & Dakin, 2010; Goffaux & Greenwood, 2016; Pachai et al., 2018). When faces are filtered in the Fourier domain to preserve only a restricted range of orientations (as in Fig. 1A), identity recognition performance at fixation typically follows a bell-shaped curve with the best identity recognition performance for horizontally filtered faces and worst performance for vertically filtered faces (Dakin and Watt, 2009; Goffaux & Greenwood, 2016; this effect is schematized in Fig. 1-B). This horizontal tuning for identity recognition has been replicated across a range of manipulations of the orientation content: not only by simple filtering or manipulation of the oriented filter bandwidths (Dakin & Watt, 2009; Goffaux, 2019; Goffaux et al., 2016; Goffaux &

Dakin, 2010; Goffaux & Greenwood, 2016; Pachai et al., 2018), but also by masking (Goffaux & Dakin, 2010; Pachai et al., 2013), notch phase scrambling (Jacques et al., 2014), and ‘bubbles’ sampling (Duncan et al., 2019). The neural signatures of face processing are also mostly driven by the horizontal face content (Goffaux et al., 2016; Jacques et al., 2014).

Importantly, there is increasing evidence that the horizontal tuning of face identification is specific to face recognition, and that it is not present at early stages of visual processing (Goffaux, 2019; Goffaux & Dakin, 2010; Goffaux & Greenwood, 2016; Jacobs et al., 2020). For instance, a recent study found distinct patterns of orientation selectivity in a low-level contrast detection task and an identification task for the same face stimuli (Jacobs et al., 2020). Moreover, the horizontal tuning of face identification is robust as long as the face stimulus is in a typical upright position, but if the face is flipped upside down, the horizontal tuning decreases, or is even absent (Fig. 1B; Goffaux, 2019; Goffaux & Dakin, 2010; Goffaux & Greenwood, 2016). Although face inversion does not remove any information from the stimulus, it is known to dramatically disrupt the high-level visual mechanisms specialized for identity recognition. Therefore, the vulnerability of horizontal tuning to inversion provides a key measure of the relevance of horizontal cues for high-level face recognition (e.g., Goffaux & Dakin, 2010; Goffaux & Greenwood, 2016; Pachai et al., 2013).

Because face recognition is horizontally-tuned, we predict that it is affected by the radial position in the peripheral visual field. In other words, the radial position of the face in the visual field should act like a natural, internal orientation filter due to the radial biases of the observer (see Fig. 1-A). Here, we reasoned that any difference in the face inversion effect (i.e., the superior ability to identify a face when it is presented upright compared to when it is inverted) between isoecentric radial locations should reflect the influence of the radial bias on the high-level mechanisms specialized for face recognition. Meanwhile, the use of inversion also allows us to control for general low-level variations in the visual field unrelated to high-level face-specialized processing (e.g. the horizontal-vertical anisotropy). Importantly, our approach does not rely on the direct manipulation of stimulus orientation content; rather, we use broadband face stimuli and utilise radial filtering that naturally operates in the visual system of the observer.

We report two variants of the same experiment, performed by separate groups of participants. Each probed only two isoecentric positions to achieve a large number of trials while keeping testing time comfortable (the left horizontal and upper vertical meridians were tested in one group, and the right horizontal and lower vertical meridians were tested in the other group). We looked at how the inversion effect varied across meridians. If high-level face recognition is

influenced by radial biases, then the effect of face inversion should be larger on the horizontal compared to vertical meridian. We observed radial influences on the face inversion effect that are consistent with this prediction both at the population level and at the individual participant level, suggesting that the high-level mechanisms specialized for face recognition are more engaged on the horizontal meridian than on the vertical meridian. Our results are consistent with the hypothesis that the radial bias modulates high-level recognition.

Method

Participants

In total, 40 young adults completed the experiment. They were naïve as to its purpose. All participants had normal or corrected-to normal visual acuity (logMAR 0.00 or better), as measured with the automated Landolt C test of the Freiburg Visual Acuity Test software (Bach, 2007). They gave their informed written consent before participating in the experiment, which was carried out in accordance with the Code of Ethics of the World Medical Association (Declaration of Helsinki) and was approved by the local ethical committee (Psychological Sciences Research Institute, UC Louvain). Participants received a monetary compensation of 8 euros per hour. Twenty participants were tested on the left horizontal meridian and the upper vertical meridian (Left-Up group, 18 women, mean age = 21.5 ± 1.9 years old), and twenty others were tested on the right horizontal meridian and the lower vertical meridian (Right-Low group)¹.

Stimuli

Stimuli consisted of front-facing photographs of three male faces and three female faces with a neutral expression, forming two triads of faces (see Fig. 2-A). Models on the photographs were young adult students and alumni (aged 18–25 years) of the Université Catholique de Louvain (Belgium), who gave written consent for the use of their image (Laguesse et al., 2012).

An elliptical aperture was superimposed on each face to remove any identity cues from outside of the face area, with each elliptical face resized to 140×193 pixels. Around the elliptical aperture, the pixels were padded with grey values (at the mean luminance of the monitor). The intensity values of the images were linearized to correct for the gamma function of the monitor. The luminance and contrast of the resulting pixel values were adjusted to obtain a mean luminance of

¹ Age and gender information of participants of group Right-low were lost, but the demographics were very similar to those of participants of group Left-up (i.e., undergrads students of about 20 years old, mostly women).

39.72 cd/m² and a root-mean-square contrast 0.07 in 0-1-pixel value. Pilot data showed that this contrast value warranted sufficient stimulus visibility in the periphery. These corrected face images were used during the Familiarisation phase (see Procedure below).

Stimuli used during the practice phase and the main experiment were varied in visibility, which allow us to measure identification performance ranging from barely visible to clearly visible. To manipulate visibility, we varied the phase coherence of the face image by parametrically randomizing image the phase structure of the images in the Fourier domain. This procedure progressively disrupts the shape of the face and its features while preserving the amplitude spectrum of the original face image. Phase-scrambled images were created using Ales et al. (2012)'s MATLAB function (phaseScrambleImage.m). Since manipulations in the Fourier domain operate on the whole image (face and background), the presence of a uniform background artificially increases the low spatial frequency energy of scrambled images. To counteract this effect, we employed the iterative scrambling procedure proposed by Petras et al. (2019), which involves repeatedly scrambling the phase of the image and pasting the original face pixels back onto the phase-scrambled image over 100 iterations. In the resulting image, the background region generated by the iterative procedure had a similar power spectrum to the face region. From there, the elliptical face region of these images was parametrically scrambled to create images with seven levels of phase coherence, linearly ranging from 0 to 90%. We did not use 100% coherent images as a pilot experiment indicated that 90% phase coherence was sufficient to elicit high recognition accuracy (ceiling performance for upright faces seen foveally). An elliptical mask was again superimposed on the filtered version of each face to create the final stimuli with a grey uniform background (see face "Rosie" in Fig. 2-A as an example). We also built a mask to prevent retinal persistence for briefly presented stimuli. The mask was a patch of $1/f$ spatial noise with a spectral slope of -2, and of the same global luminance and RMS contrast as the faces. It was presented in a circular window of 248 pixels of diameter, whose edges were cosinusoidally modulated within a transition band of 41 pixels. Faces were presented upright and inverted (i.e., vertically flipped). Inverted faces were generated by vertically flipping all face images around the suborbital region. This way both the eye and the whole face regions fell at a similar eccentricity across upright and inverted conditions (8° of visual angle). This control is important when measuring the inversion effect along the vertical meridian.

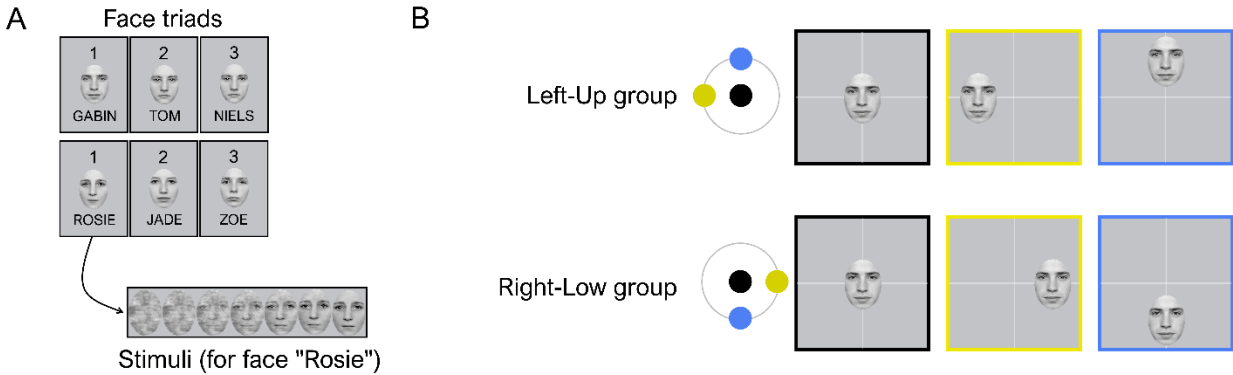


Figure 2. A. Face triads used in the experiment. Half of the participants of each group were familiarised and tested with the male triad, and the other half with the female triad. An example of the seven phase-coherence variations tested is shown with face “Rosie”. **B.** In a first group of participants (Left-Up group), the stimulus was randomly presented on each trial either to the fovea, on the left horizontal meridian, or on the upper vertical meridian, while in a second group (Right-Low group) it was randomly presented either to the fovea, on the right horizontal meridian, or on the lower vertical meridian. Stimuli were one of the three faces of the triad with which the observer had been previously familiarized. It was presented either upright or inverted at one of the seven phase-coherence levels. The luminance of the stimuli and background has been increased in this figure for better visibility.

Procedure

The experiment was programmed in E-Prime 2.0. Stimuli were viewed from a distance of 55 cm on a VIEWpixx monitor (VPixx Technologies Inc., Saint-Bruno, Canada) with a 1920 × 1080 pixels resolution and a 70Hz refresh rate. At this distance, face sizes were 5° of visual angle horizontally and 6.9° vertically (Fig. 2-B), with the mask covering 9° diameter (with a fading transition 1.5° wide). Each participant performed three experimental sessions, for a total duration around four hours. Participants sat in a darkened testing box with light absorbing black painted walls. Their head was supported with a chinrest to maintain eye-monitor distance, and they had to maintain fixation on a central fixation point. The experiment was designed to strongly discourage participants from making eye movements. In each trial, the face appeared randomly either in the fovea or at one peripheral position, in order to prevent the possibility of saccades being planned before stimulus presentation. Face stimuli remained on the screen for only 150ms. This duration corresponds approximatively to the mean saccade latency measured under time pressure (Crouzet et al., 2010; Kauffmann et al., 2019), meaning that the stimulus would disappear before eye movements could be completed. This combination of unpredictability and brief durations made eye movements during the task counterproductive. Each participant was assigned one of the face triads as stimuli (the male triad for half of the participants of each

experimental group and the female triad for the other half). Participants underwent a familiarisation phase, a practice phase and the main experiment in each of the three experimental sessions.

In the familiarisation phase, participants were first familiarised with the three identities from their assigned face triad. Faces were presented at full phase-coherence next to each other. They were associated with a number that corresponded to the response key, and with a first name in order to facilitate the familiarisation process (Fig. 2-A). The participant was instructed to look attentively at the faces in order to be able to recognize their identities later. When they felt sufficiently confident, they could move to the next step where the faces were presented individually. The participant was instructed to fixate a foveal fixation target. On each trial, one of the three faces was randomly presented to the fovea, with the participant instructed to use a numeric keypad to press the response key (1, 2, or 3) corresponding to the identity. The stimuli remained on the screen until the participant gave their response. When responses were at least 90% correct (chance level: 33%) in two consecutive blocks (42 trials), the participants performed new blocks in which the faces were randomly presented at the two peripheral locations (left and upper or right and lower visual field depending on their experimental group), remaining on the screen until a response was made, until they again reached 90% correct at both peripheral positions in two consecutive blocks.

In the subsequent practice phase, participants were trained to perform the 3AFC identity task with the phase-scrambled stimuli and task conditions used in the main experiment. Each trial was as follows: A fixation cross was displayed for a duration that varied across trials from 500 to 700ms. A single face stimulus was then displayed for 150ms. The stimulus was randomly sampled from one of the seven phase-coherence levels, and was either presented upright or inverted, at one of the three possible visual field locations (fovea, horizontal meridian, and vertical meridian). The stimulus was followed by a mask (the circular $1/f$ noise pattern whose edges smoothly blended into the background) for 500ms, then by a grey background 1100ms interval during which participants gave the response. They were instructed to favour accuracy over response time. Accuracy was calculated over blocks of 42 trials and the practice was considered sufficient when they were able to reach at least 75% of correct responses at fovea, and 50% at each peripheral position.

Finally, the participant could begin the main experiment, where trials had the same structure as the practice phase. During the main experiment of each of the three experimental sessions, they performed 21 blocks of 42 trials in total. At the end, this resulted in 63 trials per experimental

condition (441 when aggregated across the seven phase-scrambling levels). Only data from the main experiment were analysed.

Data analysis

Raw data and analysis code are available at <https://doi.org/10.17605/OSF.IO/9VUT4> (Roux-Sibilon et al., 2023). The same approach was used to analyse data from both groups of participants (Left-Up group and Right-Low group). First, we analysed accuracy data with generalized linear mixed-effects models (GLMMs). GLMMs take the whole dataset as input (i.e., accuracy for each trial of each participant) and simultaneously estimate the effects at the population level (fixed effects) and the random variability of these effects across different participants or stimuli (random effects). This multi-level structure enables the robust estimation of both population-level and individual-level parameters (see e.g., Moscatelli et al., 2012; Yu et al., 2022). The increase of recognition accuracy as a function of stimulus coherence was sigmoidal. We therefore used logistic GLMMs, with a probit link function and a lower asymptote at chance level (33% for this 3AFC design) to fit the data. We first fitted a GLMM to each group's dataset with the full interaction between phase coherence (seven levels from 0% to 90%), planar orientation (upright, inverted), and visual field position (fovea, horizontal meridian, vertical meridian) as fixed effects (see Fig. 3-A and -B). Then, similar models were fitted to data from each visual field position to test for the effect of planar orientation on the phase-coherence slope (i.e., the face inversion effect at each position). Finally, a model was fitted to peripheral data only, to test for the critical interaction between planar orientation and visual field location (i.e., the radial modulation of the face inversion effect). Each of these models included random effects to allow both the intercept and slopes for different predictors to vary across participants and face triads. The fixed and random effect structure of each model is described in detail in Table 1. GLMMs were fitted using maximum likelihood estimation and p-values were derived with Satterthwaite approximation for degrees of freedom (Luke, 2017). The significance of the effects was decided at a threshold $\alpha = 0.05$. All analyses were performed in R. Models were fitted using the lme4 package (Bates, Mächler, Bolker, & Walker, 2015) and tested with the lmerTest package (Kuznetsova et al., 2017)².

In order to get an appreciation of the extent to which the radial modulation effect was present across individuals, we additionally analysed the effect in each participant. We extracted the

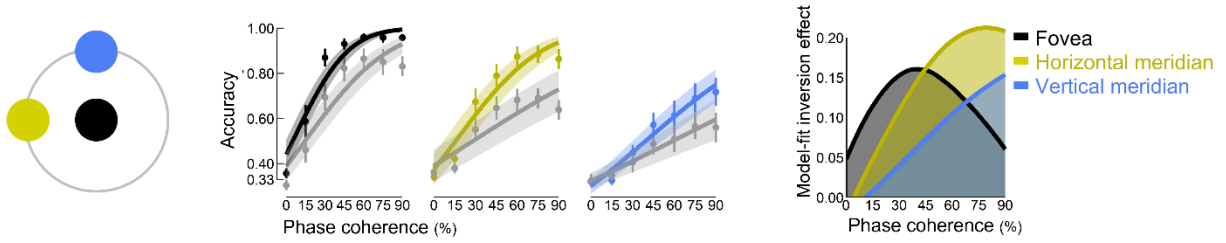
² The effects were also tested using a model comparison approach (e.g., Judd et al., 2017), which produced the same results in terms of significance. For clarity, we do not report this analysis here, but the model comparisons are available in the R analysis script at <https://doi.org/10.17605/OSF.IO/9VUT4>.

parameter estimates given by the model for the random effects using the *coef* method for GLMM (lme4 package) and used them to calculate the slopes (β parameter) of the logistic function that linked recognition performance to phase coherence for each individual and condition. The slope β reflects how much the sensitivity to face identity grows as face visibility increases in each condition (upright and inverted faces, on the horizontal and vertical meridian). For each meridian, we calculated the inversion effect as the difference between β for upright faces and β for inverted faces.

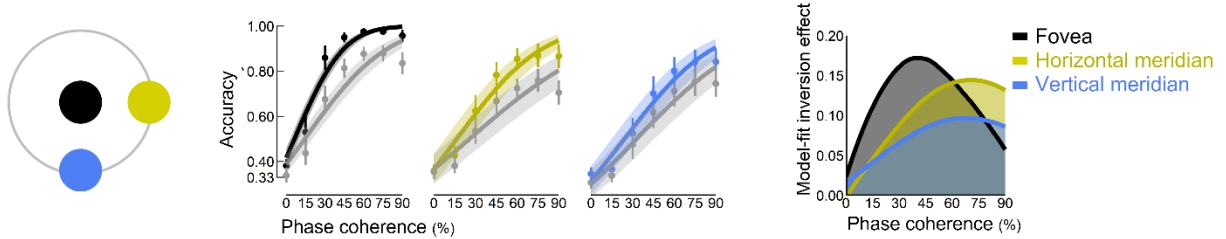
Results

Inversion effect. Figure 3 A (Left-Up group) and B (Right-Low group) show the group-averaged proportion correct values for face identification as a function of phase coherence in each condition and group (middle panel), as well as the face inversion effect quantified as the difference between the model predicted values for upright and inverted faces at each phase-coherence level (right panel). Performance in the identification task increased with phase coherence (as sensory evidence increased), following a sigmoidal shape. The population-level predictions of the logistic GLMM in each group (models A and F in Table 1) are plotted in Figure 3-A and -B. Model fits for the foveal position were noticeably similar across groups, suggesting that their face recognition abilities were comparable at fixation. Across all locations, sensitivity to face identity increased more quickly with phase coherence for upright faces compared to inverted faces in agreement with past evidence that inversion substantially hampers face identification. This inversion effect was significant for the three visual field positions in both groups (cf. models B, C, D, G, H, and I in Table 1; Left-Up group: Fovea $z = 7.68, p < .001$, Horizontal meridian $z = 9.95, p < .001$, Vertical meridian $z = 3.57, p < .001$; Right-Low group: Fovea $z = 6.28, p < .001$, Horizontal meridian $z = 8.70, p < .001$, Vertical meridian $z = 3.28, p < .001$).

A Left-up Group



B Right-low Group



C

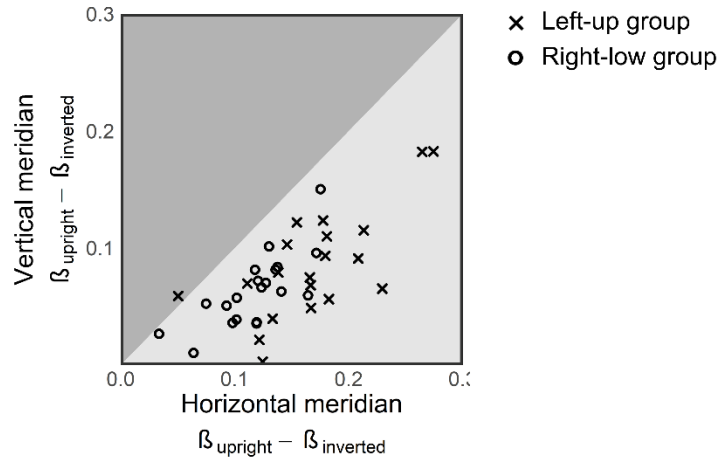


Figure 3. A. and B. Left: Stimulus locations for each group. Middle: Accuracy data averaged across participants with 95% confidence intervals (dots and error bars), on which population level predictions of the fitted GLMM are plotted with 95% confidence intervals (lines and shaded areas), in colour for upright faces and in grey for inverted faces. The horizontal axis shows the level of phase coherence of the face stimuli, from 0% (fully scrambled face) to 90% (face is well visible). The inversion effect is significant at each visual field position in each group. Importantly, it is larger on the horizontal meridian than on the vertical meridian. Right: Model-fit inversion effects, calculated as the upright-inverted difference of model estimates, as a function of phase coherence at each location. **C.** Radial modulation of the inversion effect at the individual participant level, as estimated by the difference in slope (β) between the upright and inverted conditions for the horizontal versus vertical meridian.

Radial modulation of the inversion effect. The visual inspection of Figure 3-A and B suggests that the face inversion effect is larger on the horizontal meridian compared to the vertical meridian (i.e., the difference between upright and inverted conditions is greater on the horizontal meridian). To test the significance of this critical interaction, we set aside foveal data and fitted GLMMs again (models E and J in Table 1). The interaction between phase coherence, inversion and visual field was significant in both groups (Left-Up group: $z = 2.77, p < .01$; Right-Low group: $z = 2.66, p < .01$), demonstrating that the inversion effect is indeed stronger when faces appear on the horizontal than the vertical meridian. It can also be noticed that accuracy on the lower vertical meridian (in the Right-Low group) is overall better than it is on the upper vertical meridian (in the Left-Up group), in line with the vertical meridian anisotropy (Abrams et al., 2012). Furthermore, on the horizontal meridian, the inversion effect looks more pronounced in the left visual field (Left-Up group, Fig. 3A) than it is in the right visual field (Right-Low group, Fig. 3B).

To add to the data representation, the inversion effect, calculated by subtracting model-fit accuracy for inverted faces from that for upright faces (from models A and F in Table 1), was plotted as a function of phase coherence in the right-most panel of Figure 3-A and B. The size of the inversion effect rises most rapidly in the fovea, indicating that even low amounts of sensory evidence (phase coherence) can trigger face-specialised mechanisms. This rate of increase was slower in peripheral vision, though clearly faster in the horizontal meridian than on the vertical meridian. Therefore, this result shows that the high-level specialized mechanisms recruited for the identification of faces were influenced by the radial position of the face in peripheral vision.

Radial modulation at the individual-participant level. We next extracted the random effects to calculate the phase coherence regression slope (β) in each condition for each individual participant, i.e., the slope of the psychometric function. We calculated the face inversion effect in each participant by subtracting upright from inverted slope values. In Figure 3-C, we plotted an index of the radial modulation of the inversion effect, i.e., the inversion effect on the horizontal meridian (x axis) against the inversion effect on the vertical meridian (y axis). If a participant's identity recognition mechanisms are not influenced by the radial position, their radial modulation index should fall on the diagonal. If they are influenced by the radial position, the index should fall below the diagonal, with distance to the diagonal reflecting the extent of the radial influence. Remarkably, all individual indices except for one fall below the diagonal, indicating that the inversion effect is larger on the horizontal than the vertical meridian in almost all observers.

Table 1. Results of the generalized linear mixed-effects models (GLMM). The lme4 syntax of each model is provided, with fixed effects highlighted in bold. For example, models A and F estimate the full interaction between phase coherence, planar orientation, and visual field position as fixed effects. The random effect part, in italics, means that the model estimates the intercept and the slopes for the main effects of the three predictors (phase coherence, inversion, and position) for each participant. The fact that participants were attributed two different face triads as stimuli was also considered by including the face triad as a nested random effect. β is the regression slope, i.e., the population-level parameter of the interaction being tested (the larger it is, the larger the effect).

| Model | lme4 syntax | Test |
|---|--|---|
| Left-Up group | | |
| A Full model | accuracy ~ phase coherence * planar orientation * position + (1 + <i>phase coherence</i> + planar orientation + position triad / participant) | \emptyset (Visualisation only; see Fig. 3-A) |
| B Inversion effect - fovea data only | accuracy ~ phase coherence * planar orientation + (1 + <i>phase coherence</i> * planar orientation triad / participant) | $\beta = 0.17, z = 7.68, p = 1.59e-14$ |
| C Inversion effect - left horizontal meridian data only | accuracy ~ phase coherence * planar orientation + (1 + <i>phase coherence</i> * planar orientation triad / participant) | $\beta = 0.16, z = 9.95, p = 2e-16$ |
| D Inversion effect - upper vertical meridian data only | accuracy ~ phase coherence * planar orientation + (1 + <i>phase coherence</i> * planar orientation triad / participant) | $\beta = 0.09, z = 3.57, p = 0.0004$ |
| E Critical interaction - radial effect, peripheral data only | accuracy ~ phase coherence * planar orientation * meridian + (1 + <i>phase coherence</i> * planar orientation * meridian triad / participant) | $\beta = 0.08, z = 2.77, p = 0.00$ |
| Right-Low group | | |
| F Full model | accuracy ~ phase coherence * planar orientation * position + (1 + <i>phase coherence</i> + planar orientation + position triad / participant) | \emptyset (Visualisation only; see Fig. 3-A) |
| G Inversion effect - fovea data only | accuracy ~ phase coherence * planar orientation + (1 + <i>phase coherence</i> * planar orientation triad / participant) | $\beta = 0.21, z = 6.28, p = 3.38e-10$ |
| H Inversion effect - right horizontal meridian data only | accuracy ~ phase coherence * planar orientation + (1 + <i>phase coherence</i> * planar orientation triad / participant) | $\beta = 0.11, z = 8.70, p = 2e-16$ |
| I Inversion effect - lower vertical meridian data only | accuracy ~ phase coherence * planar orientation + (1 + <i>phase coherence</i> * planar orientation triad / participant) | $\beta = 0.06, z = 3.28, p = 0.001$ |
| J Critical interaction - radial effect, peripheral data only | accuracy ~ phase coherence * planar orientation * meridian + (1 + <i>phase coherence</i> * planar orientation * meridian triad / participant) | $\beta = 0.05, z = 2.66, p = 0.008$ |

Discussion

In low-level vision, the encoding of visual information is biased towards radial orientations, with physiological correlates evident from the retina to the mid-level visual cortex. Here we provide the first evidence that the radial bias also impacts higher-level vision. We used face identity recognition as a framework, as it heavily relies on the horizontally oriented signal (Dakin & Watt, 2009; Duncan et al., 2019; Goffaux & Greenwood, 2016). Specifically, the face inversion effect, a marker of the specialized processing of faces, is larger when identity recognition is based on the horizontal cues in comparison to the vertical cues (e.g. with horizontally filtered vs vertically filtered face images; Goffaux & Greenwood, 2016; Goffaux & Dakin, 2010; Pachai et al., 2013).

This horizontal dependence of the face inversion effect indicates that the horizontal tuning of face identity recognition occurs at high-level face-specialized recognition stages of the visual processing, which enabled us to test whether the radial bias influences visual processing at these high levels. Furthermore, using a relative measure such as the inversion effect made it possible to control for other systematic asymmetries of peripheral sensitivity, which add to the radial bias (namely, the horizontal-vertical anisotropy; Barbot et al., 2021; Himmelberg et al., 2020).

We predicted and found that the inversion effect is larger on the horizontal meridian – where horizontal cues align with the radial bias – than on the vertical meridian. This result suggests that face-specialized mechanisms are modulated by the radial bias in peripheral vision. The radial influence on face-specialized processing was robustly significant in both replications of the experiment, as well as being consistent at the individual level. While the size of the radial influence varied between individuals (Fig. 3-B), the inversion effect was indeed larger on the horizontal than vertical meridian in all but one, suggesting that the effect of the radial bias on face identification may be as systematic as its effects on sensitivity to basic stimuli.

While our findings suggest that the radial bias persists at high-level stages of the ventral visual processing, the underlying mechanisms are unclear. As raised in the Introduction, this pattern may arise from an early “radial filter”, with a passive propagation of radially filtered low-level signals to higher level processing stages. From this perspective, the input is filtered by lower-level stages of processing (e.g. radially biased receptive fields in the retina and V1), and then transmitted to unbiased (i.e., circular) receptive fields in face selective areas. The stronger activation of face selective mechanisms on the horizontal meridian would be due to the horizontal signal being better represented by biased populations of upstream neuronal populations, which then carries through face selective areas. Another possibility is that high-level face-selective neurons not only passively inherit the radially biased signals from low-level, but also actively maintain some of the spatial selectivity of lower-level neurons, such as the radial bias. For example, receptive fields in face-specialized cortical regions could be radially elongated and therefore more tuned to horizontal face content on the horizontal meridian. Whether the shape of receptive fields in high-level regions is circular or preserve radial ellipticity is, to our knowledge, unknown. Population receptive field mapping studies of the category-selective visual cortex (Finzi et al., 2021; Majima et al., 2017; Poltoratski et al., 2021) typically estimate the size and position of these high-level receptive fields, but not their shape. Therefore, the possibility of the radial bias being a property of neurons up to cortical areas involved in visual recognition is yet to be explored.

The inversion effects measured in our study fit with evidence from prior studies to show that face-selective mechanisms operate in the peripheral visual field (Canas-Bajo & Whitney, 2022; Farzin et al., 2009; Kovács et al., 2017; McKone, 2004). However, these prior studies have only presented faces along the horizontal meridian. Our results rather paint a picture of differential activation of specialized mechanisms in response to the radial location of faces within the visual field. Note that in our data, the inversion effect was attenuated on the vertical meridian but nonetheless significant, indicating that face selective mechanisms are not completely turned off on the vertical meridian, at least at eccentricities like those tested here (8°). This echoes what happens in the fovea: with vertically filtered face images, the inversion effect is strongly reduced, but can still be observed (e.g. Goffaux & Greenwood, 2016). At larger eccentricities than that tested here, the effect of the radial bias on face recognition may be more dramatic. The precise location of stimuli in the visual field relative to the radial bias thus needs to be considered when designing studies of peripheral face processing. For example, the effect of the radial bias may modulate peripheral face detection. A wealth of studies have demonstrated that peripheral faces are detected rapidly and trigger ultra-fast (100-150ms) and involuntary eye-movements, compared to other categories of objects such as animals or vehicles (Boucart et al., 2016; Crouzet et al., 2010; Guyader et al., 2017; Kauffmann et al., 2019; Martin et al., 2018). However, these studies usually present peripheral faces laterally, i.e., along the horizontal meridian. Our results imply that the radial bias may have a role in triggering ultra-fast saccades towards faces, especially at large eccentricities, where the radial bias is stronger (e.g. Rovamo, 1982; Greenwood et al. 2017).

Although our study was not designed to examine hemifield differences, we also noticed that, along the horizontal meridian, the inversion effect was more pronounced in the left visual field (Left-Up group) than it was in the right visual field (Right-Low group). This asymmetry could reflect the right hemispheric lateralization of face specialized processing (e.g. Barton, 2008; Cohen et al., 2019; Hillger & Koenig, 1991). Alternatively, this asymmetry could be due to a stronger radial bias in the left than in the right hemifield, as suggested in prior studies measuring radial bias with low-level tasks (Sasaki et al. 2006; Rovamo et al. 1982; Greenwood et al. 2017; Berardi & Fiorentini 1991). Accordingly, a large scale study has demonstrated stronger crowding in the left compared to the right visual field (Kurzawski et al., 2021), which may also derive from the left-right asymmetry in the strength of the radial bias, given that crowding is stronger in the radial direction (Toet & Levi, 1992). It is therefore an intriguing possibility that hemifield variations in the radial bias may contribute to the right hemispheric lateralization of face processing.

The variability in the radial effect observed across participants (cf. Fig. 4-B) may be partly imputable to systematic idiosyncratic factors, both at the cortical and non-cortical levels. At the

level of the eye, the radial bias may be modulated by factors such as myopia, which results from the elongation of the ocular globe along the anterior-posterior axis. Vera-Diaz et al. (2005) showed that axial length (the distance from the cornea to the retina), correlated positively with low-level psychophysical measures of the radial bias, suggesting that the abnormal stretching of the retina during the development of myopic eyes results in a more pronounced radial bias than in emmetropes. Although inclusion in our study required normal or corrected-to-normal visual acuity, we did not collect optometric data. The samples may have been partly composed of (corrected) myopic observers, contributing to the variability in our data. Beyond the retina, inter-individual variability in cortical receptive fields may also have contributed to our data. For example, V1 population receptive field sizes predict individual differences in size perception (Moutsiana et al., 2016), while differences in the cortical magnification in V1 predict susceptibility to visual illusions (Schwarzkopf & Rees, 2013). Data from Merkel et al. (2018) suggests that the variability in population receptive field ellipticity is at least as important, if not more so, than the variability in their size. Finally, inter-individual variability may also result from differences in the way individuals use the horizontal cues in the face stimulus to recognize identity (Duncan et al., 2019; Goffaux et al., 2015; Goffaux & Dakin, 2010; Pachai et al., 2013). The radial bias may modulate peripheral face recognition more strongly in those with a strong horizontal preference in the fovea. A combination of the above factors could collectively drive the individual differences we observe.

In conclusion, this study demonstrates that the face inversion effect is stronger on the horizontal than on the vertical meridian, suggesting that the radial bias modulates the specialized mechanisms involved in face identity recognition in peripheral vision. This is the first evidence that the radial bias impacts human vision up to higher levels of processing by restricting the access to the orientation content of broadband ecological stimuli such as faces. The pronounced radial anisotropy of peripheral vision must be considered when examining visual recognition and other functions of high-level vision. Our observation of a radial bias for face recognition suggests that radially filtered signals are propagated throughout the visual hierarchy from low- to high-level vision, and opens the possibility that the receptive fields of neurons in high-level visual regions are also radially elongated.

Acknowledgments

We thank H el ene Dumont, Charlotte Raskopf and Salom e Rolland for their help with data acquisition. This work was supported by a graduate school travel grant from Universit e Grenoble

Alpes awarded to A.R.S. in the framework of the “Investissements d’avenir” program (ANR-15-IDEX-02), and by an Excellence of Science grant awarded to V.G. (HUMVISCAT-30991544)

References

- Abrams, J., Nizam, A., & Carrasco, M. (2012). Isoeccentric locations are not equivalent: The extent of the vertical meridian asymmetry. *Vision Research*, *52*(1), 70-78.
<https://doi.org/10.1016/j.visres.2011.10.016>
- Ales, J. M., Farzin, F., Rossion, B., & Norcia, A. M. (2012). An objective method for measuring face detection thresholds using the sweep steady-state visual evoked response. *Journal of Vision*, *12*(10), 18-18. <https://doi.org/10.1167/12.10.18>
- Bach, M. (2007). The Freiburg Visual Acuity Test-Variability unchanged by post-hoc re-analysis. *Graefe's Archive for Clinical and Experimental Ophthalmology*, *245*(7), 965-971.
<https://doi.org/10.1007/s00417-006-0474-4>
- Baden, T., Euler, T., & Berens, P. (2020). Understanding the retinal basis of vision across species. *Nature Reviews Neuroscience*, *21*(1), 5-20. <https://doi.org/10.1038/s41583-019-0242-1>
- Barbot, A., Xue, S., & Carrasco, M. (2021). Asymmetries in visual acuity around the visual field. *Journal of Vision*, *21*(1), 2. <https://doi.org/10.1167/jov.21.1.2>
- Barton, J. J. S. (2008). Structure and function in acquired prosopagnosia: Lessons from a series of 10 patients with brain damage. *Journal of Neuropsychology*, *2*(1), 197-225.
<https://doi.org/10.1348/174866407X214172>
- Bates, D., Mächler, M., Bolker, B., & Walker, S. (2015). Fitting Linear Mixed-Effects Models Using **lme4**. *Journal of Statistical Software*, *67*(1). <https://doi.org/10.18637/jss.v067.i01>
- Bennett, P. J., & Banks, M. S. (1991). The effects of contrast, spatial scale, and orientation on foveal and peripheral phase discrimination. *Vision Research*, *31*(10), 1759-1786.
[https://doi.org/10.1016/0042-6989\(91\)90025-Z](https://doi.org/10.1016/0042-6989(91)90025-Z)
- Berardi, N., & Fiorentini, A. (1991). Visual field asymmetries in pattern discrimination: A sign of asymmetry in cortical visual field representation? *Vision Research*, *31*(10), 1831-1836.
[https://doi.org/10.1016/0042-6989\(91\)90030-9](https://doi.org/10.1016/0042-6989(91)90030-9)
- Boucart, M., Lenoble, Q., Quettelart, J., Szaffarczyk, S., Desprez, P., & Thorpe, S. J. (2016). Finding faces, animals, and vehicles in far peripheral vision. *Journal of Vision*, *16*(2), 10.
<https://doi.org/10.1167/16.2.10>
- Canas-Bajo, T., & Whitney, D. (2022). Relative tuning of holistic face processing towards the fovea. *Vision Research*, *197*, 108049. <https://doi.org/10.1016/j.visres.2022.108049>
- Cohen, A. L., Soussand, L., Corrow, S. L., Martinaud, O., Barton, J. J. S., & Fox, M. D. (2019). Looking beyond the face area: Lesion network mapping of prosopagnosia. *Brain*, *142*(12), 3975-3990.
<https://doi.org/10.1093/brain/awz332>
- Crouzet, S. M., Kirchner, H., & Thorpe, S. J. (2010). Fast saccades toward faces: Face detection in just 100 ms. *Journal of Vision*, *10*(4), 1-17. <https://doi.org/10.1167/10.4.16>
- Dakin, S. C., & Watt, R. J. (2009). Biological « bar codes » in human faces. *Journal of Vision*, *9*(4), 2-2.
<https://doi.org/10.1167/9.4.2>

- Davey, M. P., & Zanker, J. M. (1998). Detecting the orientation of short lines in the periphery. *Australian and New Zealand Journal of Ophthalmology*, *26*, S104-S107. <https://doi.org/10.1111/j.1442-9071.1998.tb01354.x>
- DiCarlo, J. J., Zoccolan, D., & Rust, N. C. (2012). How Does the Brain Solve Visual Object Recognition? *Neuron*, *73*(3), 415-434. <https://doi.org/10.1016/j.neuron.2012.01.010>
- Duncan, J., Royer, J., Dugas, G., Blais, C., & Fiset, D. (2019). Revisiting the link between horizontal tuning and face processing ability with independent measures. *Journal of Experimental Psychology: Human Perception and Performance*, *45*(11), 1429-1435. <https://doi.org/10.1037/xhp0000684>
- Farzin, F., Rivera, S. M., & Whitney, D. (2009). Holistic crowding of Mooney faces. *Journal of Vision*, *9*(6), 18-18. <https://doi.org/10.1167/9.6.18>
- Finzi, D., Gomez, J., Nordt, M., Rezai, A. A., Poltoratski, S., & Grill-Spector, K. (2021). Differential spatial computations in ventral and lateral face-selective regions are scaffolded by structural connections. *Nature Communications*, *12*(1), 2278. <https://doi.org/10.1038/s41467-021-22524-2>
- Goffaux, V. (2019). Fixed or flexible? Orientation preference in identity and gaze processing in humans. *PLOS ONE*, *14*(1), e0210503. <https://doi.org/10.1371/journal.pone.0210503>
- Goffaux, V., & Dakin, S. C. (2010). Horizontal information drives the behavioral signatures of face processing. *Frontiers in Psychology*, *1*. <https://doi.org/10.3389/fpsyg.2010.00143>
- Goffaux, V., Duecker, F., Hausfeld, L., Schiltz, C., & Goebel, R. (2016). Horizontal tuning for faces originates in high-level Fusiform Face Area. *Neuropsychologia*, *81*, 1-11. <https://doi.org/10.1016/j.neuropsychologia.2015.12.004>
- Goffaux, V., & Greenwood, J. A. (2016). The orientation selectivity of face identification. *Scientific Reports*, *6*(1), 34204. <https://doi.org/10.1038/srep34204>
- Goffaux, V., Poncin, A., & Schiltz, C. (2015). Selectivity of Face Perception to Horizontal Information over Lifespan (from 6 to 74 Year Old). *PLOS ONE*, *10*(9), e0138812. <https://doi.org/10.1371/journal.pone.0138812>
- Greenwood, J. A., Szinte, M., Sayim, B., & Cavanagh, P. (2017). Variations in crowding, saccadic precision, and spatial localization reveal the shared topology of spatial vision. *Proceedings of the National Academy of Sciences*, *114*(17), E3573-E3582. <https://doi.org/10.1073/pnas.1615504114>
- Guyader, N., Chauvin, A., Boucart, M., & Peyrin, C. (2017). Do low spatial frequencies explain the extremely fast saccades towards human faces? *Vision Research*, *133*, 100-111. <https://doi.org/10.1016/j.visres.2016.12.019>
- Hillger, L. A., & Koenig, O. (1991). Separable Mechanisms in Face Processing: Evidence from Hemispheric Specialization. *Journal of Cognitive Neuroscience*, *3*(1), 42-58. <https://doi.org/10.1162/jocn.1991.3.1.42>
- Himmelberg, M. M., Winawer, J., & Carrasco, M. (2020). Stimulus-dependent contrast sensitivity asymmetries around the visual field. *Journal of Vision*, *20*(9), 18. <https://doi.org/10.1167/jov.20.9.18>
- Jacobs, C., Petras, K., Moors, P., & Goffaux, V. (2020). Contrast versus identity encoding in the face image follow distinct orientation selectivity profiles. *PLOS ONE*, *15*(3), e0229185. <https://doi.org/10.1371/journal.pone.0229185>
- Jacques, C., Schiltz, C., & Goffaux, V. (2014). Face perception is tuned to horizontal orientation in the N170 time window. *Journal of Vision*, *14*(2), 5-5. <https://doi.org/10.1167/14.2.5>

- Judd, C. M., McClelland, G. H., & Ryan, C. S. (2017). *Data Analysis: A Model Comparison Approach to Regression, ANOVA, and Beyond* (3^e éd.). Routledge. <https://doi.org/10.4324/9781315744131>
- Kauffmann, L., Peyrin, C., Chauvin, A., Entzmann, L., Breuil, C., & Guyader, N. (2019). Face perception influences the programming of eye movements. *Scientific Reports*, *9*(1), 560. <https://doi.org/10.1038/s41598-018-36510-0>
- Kovács, P., Knakker, B., Hermann, P., Kovács, G., & Vidnyánszky, Z. (2017). Face inversion reveals holistic processing of peripheral faces. *Cortex*, *97*, 81-95. <https://doi.org/10.1016/j.cortex.2017.09.020>
- Kurzawski, J. W., Burchell, A., Thapa, D., Majaj, N. J., Winawer, J. A., & Pelli, D. G. (2021). *An enhanced Bouma model fits a hundred people's visual crowding* [Preprint]. Neuroscience. <https://doi.org/10.1101/2021.04.12.439570>
- Kurzawski, J. W., Burchell, A., Thapa, D., Winawer, J., Majaj, N. J., & Pelli, D. G. (2021). *The Bouma law accounts for crowding in fifty observers* [Preprint]. Neuroscience. <https://doi.org/10.1101/2021.04.12.439570>
- Kuznetsova, A., Brockhoff, P. B., & Christensen, R. H. B. (2017). lmerTest Package: Tests in Linear Mixed Effects Models. *Journal of Statistical Software*, *82*(13). <https://doi.org/10.18637/jss.v082.i13>
- Laguesse, R., Dormal, G., Biervoye, A., Kuefner, D., & Rossion, B. (2012). Extensive visual training in adulthood significantly reduces the face inversion effect. *Journal of Vision*, *12*(10), 14-14. <https://doi.org/10.1167/12.10.14>
- Leopold, D. A., O'Toole, A. J., Vetter, T., & Blanz, V. (2001). Prototype-referenced shape encoding revealed by high-level aftereffects. *Nature Neuroscience*, *4*(1), 89-94. <https://doi.org/10.1038/82947>
- Lerma-Usabiaga, G., Winawer, J., & Wandell, B. A. (2021). Population Receptive Field Shapes in Early Visual Cortex Are Nearly Circular. *The Journal of Neuroscience*, *41*(11), 2420-2427. <https://doi.org/10.1523/JNEUROSCI.3052-20.2021>
- Leventhal, A. G. (1983). Relationship between preferred orientation and receptive field position of neurons in cat striate cortex. *The Journal of Comparative Neurology*, *220*(4), 476-483. <https://doi.org/10.1002/cne.902200409>
- Leventhal, A. G., & Schall, J. D. (1983). Structural basis of orientation sensitivity of cat retinal ganglion cells. *The Journal of Comparative Neurology*, *220*(4), 465-475. <https://doi.org/10.1002/cne.902200408>
- Leventhal, A. G., Schall, J. D., & Wallace, W. (1984). Relationship between preferred orientation and receptive field position of neurons in extrastriate cortex (area 19) in the cat. *The Journal of Comparative Neurology*, *222*(3), 445-451. <https://doi.org/10.1002/cne.902220309>
- Luke, S. G. (2017). Evaluating significance in linear mixed-effects models in R. *Behavior Research Methods*, *49*(4), 1494-1502. <https://doi.org/10.3758/s13428-016-0809-y>
- Majima, K., Sukhanov, P., Horikawa, T., & Kamitani, Y. (2017). Position Information Encoded by Population Activity in Hierarchical Visual Areas. *ENEURO*, *4*(2), ENEURO.0268-16.2017. <https://doi.org/10.1523/ENEURO.0268-16.2017>
- Malavita, M. S., Vidyasagar, T. R., & McKendrick, A. M. (2018). Eccentricity dependence of orientation anisotropy of surround suppression of contrast-detection threshold. *Journal of Vision*, *18*(7), 5. <https://doi.org/10.1167/18.7.5>

- Martin, J. G., Davis, C. E., Riesenhuber, M., & Thorpe, S. J. (2018). Zapping 500 faces in less than 100 seconds: Evidence for extremely fast and sustained continuous visual search. *Scientific Reports*, 8(1), 12482. <https://doi.org/10.1038/s41598-018-30245-8>
- McKone, E. (2004). Isolating the Special Component of Face Recognition: Peripheral Identification and a Mooney Face. *Journal of Experimental Psychology: Learning, Memory, and Cognition*, 30(1), 181-197. <https://doi.org/10.1037/0278-7393.30.1.181>
- Merkel, C., Hopf, J., & Schoenfeld, M. A. (2018). Spatial elongation of population receptive field profiles revealed by model-free fMRI back-projection. *Human Brain Mapping*, 39(6), 2472-2481. <https://doi.org/10.1002/hbm.24015>
- Merkel, C., Hopf, J., & Schoenfeld, M. A. (2020). Modulating the global orientation bias of the visual system changes population receptive field elongations. *Human Brain Mapping*, 41(7), 1765-1774. <https://doi.org/10.1002/hbm.24909>
- Moscattelli, A., Mezzetti, M., & Lacquaniti, F. (2012). Modeling psychophysical data at the population-level: The generalized linear mixed model. *Journal of Vision*, 12(11), 26-26. <https://doi.org/10.1167/12.11.26>
- Moutsiana, C., de Haas, B., Papageorgiou, A., van Dijk, J. A., Balraj, A., Greenwood, J. A., & Schwarzkopf, D. S. (2016). Cortical idiosyncrasies predict the perception of object size. *Nature Communications*, 7(1), 12110. <https://doi.org/10.1038/ncomms12110>
- Pachai, M. V., Bennett, P. J., & Sekuler, A. B. (2018). The Bandwidth of Diagnostic Horizontal Structure for Face Identification. *Perception*, 47(4), 397-413. <https://doi.org/10.1177/0301006618754479>
- Pachai, M. V., Sekuler, A. B., & Bennett, P. J. (2013). Sensitivity to Information Conveyed by Horizontal Contours is Correlated with Face Identification Accuracy. *Frontiers in Psychology*, 4. <https://doi.org/10.3389/fpsyg.2013.00074>
- Petras, K., ten Oever, S., Jacobs, C., & Goffaux, V. (2019). Coarse-to-fine information integration in human vision. *NeuroImage*, 186, 103-112. <https://doi.org/10.1016/j.neuroimage.2018.10.086>
- Petrov, Y., & McKee, S. P. (2006). The effect of spatial configuration on surround suppression of contrast sensitivity. *Journal of Vision*, 6(3), 4. <https://doi.org/10.1167/6.3.4>
- Pigarev, I. N., Nothdurft, H.-C., & Kastner, S. (2002). Neurons with radial receptive fields in monkey area V4A: Evidence of a subdivision of prelunate gyrus based on neuronal response properties. *Experimental Brain Research*, 145(2), 199-206. <https://doi.org/10.1007/s00221-002-1112-y>
- Pigarev, I. N., & Rodionova, E. I. (1998). Two visual areas located in the middle suprasylvian gyrus (cytoarchitectonic field 7) of the cat's cortex. *Neuroscience*, 85(3), 717-732. [https://doi.org/10.1016/S0306-4522\(97\)00642-8](https://doi.org/10.1016/S0306-4522(97)00642-8)
- Poltoratski, S., Kay, K., Finzi, D., & Grill-Spector, K. (2021). Holistic face recognition is an emergent phenomenon of spatial processing in face-selective regions. *Nature Communications*, 12(1), 4745. <https://doi.org/10.1038/s41467-021-24806-1>
- Riesenhuber, M., & Poggio, T. (1999). Hierarchical models of object recognition in cortex. *Nature Neuroscience*, 2(11), 1019-1025. <https://doi.org/10.1038/14819>
- Rodionova, Elena I., Revishchin, Alexander V., & Pigarev, Ivan N. (2004). Distant cortical locations of the upper and lower quadrants of the visual field represented by neurons with elongated and radially oriented receptive fields. *Experimental Brain Research*, 158(3). <https://doi.org/10.1007/s00221-004-1967-1>

- Rovamo, J., Virsu, V., Laurinen, P., & Hyvdrinen, L. (1982). Resolution of gratings oriented along and across meridians in peripheral vision. *Investigative Ophthalmology & Visual Science*, 23(5), 666-670.
- Sasaki, Y., Rajimehr, R., Kim, B. W., Ekstrom, L. B., Vanduffel, W., & Tootell, R. B. H. (2006). The Radial Bias: A Different Slant on Visual Orientation Sensitivity in Human and Nonhuman Primates. *Neuron*, 51(5), 661-670. <https://doi.org/10.1016/j.neuron.2006.07.021>
- Schall, J. D., Perry, V. H., & Leventhal, A. G. (1986). Retinal ganglion cell dendritic fields in old-world monkeys are oriented radially. *Brain Research*, 368(1), 18-23. [https://doi.org/10.1016/0006-8993\(86\)91037-1](https://doi.org/10.1016/0006-8993(86)91037-1)
- Schwarzkopf, D. S., & Rees, G. (2013). Subjective Size Perception Depends on Central Visual Cortical Magnification in Human V1. *PLoS ONE*, 8(3), e60550. <https://doi.org/10.1371/journal.pone.0060550>
- Schwarzlose, R. F., Swisher, J. D., Swisher, S., & Kanwisher, N. (2008). The distribution of category and location information across object-selective regions in human visual cortex. *Proceedings of the National Academy of Sciences*, 105(11), 4447-4452. <https://doi.org/10.1073/pnas.0800431105>
- Shou, T., Ruan, D., & Zhou, Y. (1986). The orientation bias of LGN neurons shows topographic relation to area centralis in the cat retina. *Experimental Brain Research*, 64(1). <https://doi.org/10.1007/BF00238218>
- Silson, E. H., Reynolds, R. C., Kravitz, D. J., & Baker, C. I. (2018). Differential Sampling of Visual Space in Ventral and Dorsal Early Visual Cortex. *The Journal of Neuroscience*, 38(9), 2294-2303. <https://doi.org/10.1523/JNEUROSCI.2717-17.2018>
- Smith, E. L., Chino, Y. M., Ridder, W. H., Kitagawa, K., & Langston, A. (1990). Orientation bias of neurons in the lateral geniculate nucleus of macaque monkeys. *Visual Neuroscience*, 5(6), 525-545. <https://doi.org/10.1017/S0952523800000699>
- Strasburger, H., Rentschler, I., & Jüttner, M. (2011). Peripheral vision and pattern recognition: A review. *Journal of Vision*, 11(5), 13-13. <https://doi.org/10.1167/11.5.13>
- Toet, A., & Levi, D. M. (1992). The two-dimensional shape of spatial interaction zones in the parafovea. *Vision Research*, 32(7), 1349-1357. [https://doi.org/10.1016/0042-6989\(92\)90227-A](https://doi.org/10.1016/0042-6989(92)90227-A)
- Venkataraman, A. P., Winter, S., Rosen, R., & Lundstrom, L. (2016). Choice of Grating Orientation for Evaluation of Peripheral Vision. *Optometry and Vision Science*, 93(6), 8.
- Vera-Diaz, F. A., McGraw, P. V., Strang, N. C., & Whitaker, D. (2005). A Psychophysical Investigation of Ocular Expansion in Human Eyes. *Investigative Ophthalmology & Visual Science*, 46(2), 758. <https://doi.org/10.1167/iovs.04-0127>
- Westheimer, G. (2003). The distribution of preferred orientations in the peripheral visual field. *Vision Research*, 43(1), 53-57. [https://doi.org/10.1016/S0042-6989\(02\)00398-X](https://doi.org/10.1016/S0042-6989(02)00398-X)
- Yap, Y. L., Levi, D. M., & Klein, S. A. (1987). Peripheral hyperacuity: Isoeccentric bisection is better than radial bisection. *Journal of the Optical Society of America A*, 4(8), 1562. <https://doi.org/10.1364/JOSAA.4.001562>
- Yu, Z., Guindani, M., Grieco, S. F., Chen, L., Holmes, T. C., & Xu, X. (2022). Beyond t test and ANOVA: Applications of mixed-effects models for more rigorous statistical analysis in neuroscience research. *Neuron*, 110(1), 21-35. <https://doi.org/10.1016/j.neuron.2021.10.030>
- Zheleznyak, L., Barbot, A., Ghosh, A., & Yoon, G. (2016). Optical and neural anisotropy in peripheral vision. *Journal of Vision*, 16(5), 1. <https://doi.org/10.1167/16.5.1>